A Novel Endogenous Inhibitor of Phenoloxidase from *Musca domestica* Has a Cystine Motif Commonly Found in Snail and Spider Toxins†

Alexes C. Daquinag,‡,§,|| Takashi Sato,‡,§ Haruki Koda,‡ Toshifumi Takao,⊥ Masafumi Fukuda,⊥ Yasutsugu Shimonishi,⊥ and Takuji Tsukamoto*,‡

Department of Applied Biological Sciences, Saga University, Honjomachi-1, Saga 840-8502, Japan, and Institute for Protein Research, Osaka University, Yamadaoka 3-2, Suita, Osaka 565-0871, Japan

Received August 18, 1998; Revised Manuscript Received November 19, 1998

ABSTRACT: Phenoloxidase inhibitor (POI), found in the hemolymph of housefly pupae, is a novel dopa-containing and cystine-rich peptide that competitively inhibits phenoloxidase with a K_i in the nanomolar range. [Tyr^{32}]POI is a potential precursor molecule also found in the hemolymph that may be posttranslationally oxidized to the dopa-containing peptide after creation of a rigid structure. By employing both a solid-phase peptide synthesis system based on a 9-fluorenylmethoxycarbonyl strategy and a specific air oxidation technique to ensure correct folding, we have been able to synthesize [Tyr^{32}]POI. The synthetic [Tyr^{32}]POI was confirmed to be identical to the native [Tyr^{32}]POI by coelution high-performance liquid chromatography analysis and by enzymatic analysis using the phenoloxidase inhibition assay. To determine the disulfide pairings within the peptides, a series of enzyme hydrolyses and partial reduction/alkylation steps were performed. Three cystine pairs (Cys^{11}−Cys^{25}, Cys^{18}−Cys^{29}, and Cys^{24}−Cys^{36}) were determined by identification of the resulting peptides. The disulfide pairings of the two adjacent Cys residues (Cys^{11}−Cys^{25} and Cys^{24}−Cys^{36}) were unambiguously assigned by comparing the derived fragments with the two possible isomers synthesized through a novel disulfide-linking technique. The arrangement of the disulfide bridges in POI was found to be topologically identical to those found for several peptides within the inhibitor cystine knot structural family. Although these peptides share a low primary sequence homology and display a diversity of biological functions, they nonetheless share similarities in their cystine motifs and tertiary structure. The tertiary structure model of POI, which was derived through molecular dynamics and energy minimization studies using restraints with determined disulfide connectivities, suggests that POI is a new class member of the inhibitor cystine-knot structural family.

Insect phenoloxidase (PO;[1] monophenol, dihydroxyphenylalanine:oxygen oxidoreductase; EC 1.14.18.1), also known as tyrosinase, is a widely distributed copper-containing enzyme that catalyzes two successive reactions: hydroxylation of a monophenol to *o*-diphenol and the corresponding oxidation of the *o*-diphenol to an *o*-quinone (*1*, *2*). Production of *o*-quinones by PO has been known to be an initial step in the biochemical cascade of melanin biosynthesis, a process that occupies several major roles in insect development, i.e., in cuticular tanning and sclerotization, wound healing, and defense against foreign pathogens (*3*−*6*). Thus, elucidation of the molecular mechanisms of the regulation of the PO activity, as well as those of the pro-PO activation systems (*7*−*9*), will lead to a better understanding of the physiological roles of this important enzyme system in insect development.

Recently, a unique and potent endogenous peptide inhibitor of PO activity was discovered in the hemolymph of housefly pupae (*10*). The phenoloxidase inhibitor (POI) is a basic lysine-rich peptide comprising 38 amino acid residues and a unique modified residue, dopa, at position 32 (*11*). Six Cys residues forming three intramolecular disulfide bridges in POI cluster around a region within the C-terminal two-thirds of the peptide (*11*). Although these disulfides appear to be critical in forming functionally active POI, neither the connectivities of the disulfide bridges nor the tertiary structure of POI has been examined, largely due to the low abundance of the peptide in housefly pupae.

To further investigate the structure−function relationship of POI, we first chemically synthesized [Tyr^{32}]POI, a homologue of POI in which the dopa residue at position 32

† This work was supported by Grants-in-Aid for Scientific Research from the Ministry of Education, Science and Culture of Japan, as well as the Milbon Corporation of Japan.

* To whom correspondence should be addressed: Phone +81 952 28 8775; Fax +81 952 28 8709; e-mail tsukamot@cc.saga-u.ac.jp.

‡ Saga University.

§ These two authors equally contributed to this work.

|| Present address: Department of Chemistry, Iligan Institute of Technology, Mindanao State University, Iligan 9200, Philippines.

⊥ Osaka University.

[1] Abbreviations: PO, phenoloxidase; POI, phenoloxidase inhibitor; [Tyr^{32}]POI, a homologue of phenoloxidase inhibitor with Tyr instead of dopa residue at position 32; Bis-Tris, bis(2-hydroxyethyl)iminotris-(hydroxymethyl)methane; dopa, 3,4-dihydroxyphenylalanine; Asp-N, a metalloproteinase from *Pseudomonas fragi*; LEP, a lysyl endopeptidase from *Achromobacter lyticus*; TFA, trifluoroacetic acid; DMF, *N*,*N*-dimethylformamide; HOBt, 1-benzohydroxytriazole; RP, reversed-phase; HATU, *N*-[(dimethylamino)-1*H*-1,2,3-triazol[4,5-β]pyridylmethylene]-*N*-methylmethanaminium hexafluorophosphate *N*-oxide; TBTU, 2-(1*H*-benzotriazol-1-yl)-1,1,3,3-tetramethyluronium tetrafluoroborate; Acm, acetamidomethyl; TCEP, tris(2-carboxyethyl)phosphine; ESI, electrospray ionization; MALDI-TOF, matrix-assisted laser desorption/ionization time-of-flight; HPLC, high-performance liquid chromatography; MS, mass spectrometry.

10.1021/bi9819834 CCC: $18.00
Published on Web 01/29/1999

is replaced by Tyr. This peptide, a plausible precursor molecule of POI that has been found as a minor product in the hemolymph of housefly pupae, has been suggested to be posttranslationally oxidized into mature form after its folding into a rigid structure (*11*). The peptide synthesized in this study was confirmed to be chemically and functionally identical to native peptide by the following criteria: ESI and MALDI-TOF mass spectrometry, amino acid sequence and composition analyses, coinjection HPLC analysis, and enzymatic analyses. On the basis of this peptide's structure, the disulfide pairings of [Tyr^{32}]POI were unambiguously assigned. Modeling studies through molecular dynamics simulation and energy minimization, in which restraints by disulfide linkages were taken into account, suggest that POI is a new class member of inhibitor cystine-knot structural families (*12*, *13*).

MATERIALS AND METHODS

Chemicals. *N*-(9-Fluorenyl)methyloxycarbonyl (Fmoc) amino acids included Cys(triphenylmethyl, Trt), Cys(acetamidomethyl, Acm), Arg(2,2,4,6,7-pentamethyldihydrobenzofuran-5-sulfonyl), Thr(*tert*-butyl, *t*Bu), Ser(*t*Bu), Asp(*tert*-butyl ester, O*t*Bu), Asn(Trt), Glu(O*t*Bu), Gln(Trt), Tyr(*t*Bu), His(Trt), Lys(*tert*-butyloxycarbonyl). Fmoc-Thr(*t*Bu) bound on poly(ethylene glycol)−polystyrene (PEG−PS) resin, diisopropyl ethylamine, and *N*-[(dimethylamino)-1*H*-1,2,3-triazol[4,5-β]pyridylmethylene]-*N*-methylmethanaminium hexafluorophosphate *N*-oxide (HATU, *14*) were supplied by PerSeptive Biosystems, Inc. (Framingham, MA). Low H_2O content grade of *N*,*N*-dimethylformamide (DMF) was obtained from Nacalai Tesque (Kyoto, Japan) and was used throughout the syntheses. *N*-Acetylimidazole and α-cyano-4-hydroxycinnamic acid were obtained from Watanabe Chemical Industries (Hiroshima, Japan) and Sigma Chemical Co. (St. Louis, MO), respectively. *Achromobacter lyticus* protease I (lysylendopeptidase, LEP) and endoproteinase Asp-N from *Pseudomonas fragi* were purchased from Wako Pure Chemical Industries (Osaka, Japan) and Boehringer Mannheim, respectively. Develosil, Cosmosil, and Wakosil columns were obtained from Nomura Chemical (Aichi, Japan), Nacalai, and Wako, respectively. Pico-Tag column is the product of Waters (Milford, MA). Tris(2-carboxyethyl)phosphine (TCEP) was synthesized by the method of Burns et al. (*15*). Other reagents of analytical grade are products of Nacalai Tesque and were used without further purification.

Insects. Pupae of the housefly *Musca domestica* L. were raised and collected according to our previous report (*10*).

Purification of Authentic Housefly POI. Native [Tyr^{32}]POI was purified from housefly pupae as previously described by Daquinag et al. (*11*) with the following modification. In the final step the samples were fractionated on a Develosil ODS−HG-5 column (4.6 × 150 mm) at 35 °C with a linear gradient of 5−25% acetonitrile in water in the presence of 0.1% TFA. Each analysis took approximately 40 min at a flow rate of 1 mL/min. The purified native [Tyr^{32}]POI was first identified by automatic Edman degradation analysis and ESI mass spectrometry and finally confirmed with amino acid analysis (Table 1).

Synthesis of [Tyr^{32}]POI. The linear peptide was synthesized by employing an Fmoc strategy on a continuous-flow 9050 peptide synthesizer (PerSeptive Biosystems) at 0.1 mmol scale. PEG−PS resins in which the first protected amino acid was already attached were packed in a space-adjustable column and the bed volume was continuously adjusted during the synthesis. Six equivalents of diisopropylethylamine in DMF was added to the sealed mixtures of Fmoc-protected amino acids (4 equiv) and HATU (4 equiv) for initiation of in situ activation reaction just before coupling reactions. The time and number of repetitions of these reactions were optimized for each of the steps in order to minimize the formation of defective peptides. Fmoc protecting groups were cleaved by 20% (v/v) piperidine/DMF except for the four N-terminal residues, where 25% (v/v) piperidine/DMF containing 0.1 M HOBt was used in order to minimize aspartimide formation at Asp^4 (*17*). Residual free amino termini at each coupling step were capped by 0.5 M *N*-acetylimidazole/DMF. After, the peptides synthesized on the resins (0.1 mmol) were cleaved, all protecting groups were removed, typically by the treatment with a cocktail containing TFA/thioanisole/*m*-cresol/ethane-1,2-dithiol (40:6:1:3 v/v/v/v). The reaction mixture was stirred at 0 °C for 1 h, followed by an additional 2 h at room temperature. The mixture was filtered and evaporated in vacuo. The residue was washed with diethyl ether, dried in vacuo, and dissolved in 2 mL of 80% aqueous acetonitrile containing 1% TFA. The solution was subjected to an oxidative folding reaction by dropping into degassed 100 mM Tris/acetate buffer (pH 7.5) to a final peptide concentration of 1×10^{-4} M. Degassing of the solution prior to dilution of the peptide was found to be required to remove saturating levels of molecular oxygen in the solutions, which rapidly oxidize free thiols and lead to the production of misfolded peptides. The solution was then gently stirred at 4 °C to permit moderate oxidation by oxygen in the air. The reaction was monitored by Ellman's test (*18*) and analytical RP-HPLC. After completion of the reaction, the dilute solution was continuously concentrated and desalted on parallel Cosmosil $5C_{18}$AR-300 columns (8 × 50 mm × 2) and directly separated on a Cosmosil $5C_{18}$AR-300 column (8 × 200 mm) using HPLC equipment developed for the analysis of large volumes of diluted sample (*19*). A unique major product was isolated that was further purified on a Develosil ODS−HG-5 column (8 × 150 mm).

Synthesis of Authentic Peptides for Assignment of Adjacent Disulfide Pairs. The scheme for synthesis of S1, which was used for assignment of tandem Cys residues, is shown in Figure 5. The linear peptides **1**, **2**, **3**, **4**, and **6**, used in the construction of the **S1** peptide fragment, were prepared as described in the previous section except a cocktail containing TFA (8 mL), thioanisole (1.7 mL), *m*-cresol (0.3 mL) and 2,2′-dithiodipyridine (10 equiv) was used instead of ethane-1,2-dithiol for in situ conversion of the Trt group in peptide **1** to a 2-thiopyridyl group in deprotection step. For preparation of peptide **5**, peptide **4** (5 μmol) was dissolved in 250 μL of 50 mM sodium phosphate buffer (degassed) containing 1 mM Na_2EDTA (pH 6.0). The solution of peptide **4** was dropped gradually into a solution of peptide **2** (7.5 μmol in 500 μL of the same buffer) under N_2 atmosphere and stirred for 15 min at 25 °C. The reaction mixture was separated by semipreparative HPLC and the isolated peptide **5** was lyophilized (yield 88%). For final construction of **S1**, peptide **5** (0.4 μmol) and peptide **6** (4 μmol) were dissolved together

into 250 μL of 25% CH_3OH followed by 500 μL of I_2 solution [1 M HCl/CH_3OH (1:4 v/v) containing 3.81 mg of I_2]. The mixture was vigorously stirred for 5 min at 0 °C. The reaction was quenched by the addition of saturated sodium ascorbate prior to dilution with five volumes of water. The peptides were recovered by batch absorption to 300 mg of Cosmosil 140C_{18}−OPN resin. After being washed three times with water containing 0.1% TFA, the peptides were eluted twice with 2.5 mL of 80% acetonitrile containing 0.1% TFA and lyophilized. The crude product was purified by HPLC. HPLC purification of peptides **5** and **S1** were performed on a Waters M600 multisolvent delivery system equipped with a Cosmosil 5C_{18}AR-300 column (10 × 250 mm). Samples were eluted at 45 °C with 0.1% TFA in H_2O (buffer A) and 0.1% TFA in acetonitrile (buffer B) with a flow rate of 3 mL/min. The gradients for the above separation consisted of 5% acetonitrile traversing to 20% in the first 30 min by a convex curve (number 5) followed by a 20−30% linear gradient of acetonitrile for the next 20 min. Eluents were kept under a blanket of helium.

LEP Digestion of [Tyr[32]]POI. For this enzymatic digestion, 1.4 nmol of peptide was dissolved in 25 μL of 0.1 M Bis-Tris-HCl buffer (pH 5.5) containing 4 M guanidine hydrochloride. The solution was sealed under N_2 atmosphere and incubated at 70 °C for 1 h. The peptide was diluted with 75 μL of the above buffer and digested by addition of 1 μL of LEP solution (0.1 μg/1 μL of 0.1 M Tris-HCl, pH 8.5) to the denatured peptide solution. After incubation at 37 °C for 3 h, 100 μL of 10% TFA was added and the mixture was separated by HPLC (Figure 3). The products were identified by MALDI-TOF MS and amino acid analyses (Table 1). Conditions for the HPLC separation are shown in the Figure 3 caption.

Asp-N Digestion of LEP Digested Fragments. The K3 peptide (Figure 3, 560 pmol) remaining after LEP digestion was lyophilized and redissolved in 50 μL of 50 mM Bis-Tris-HCl (pH 6.0). After addition of 3.7 μL of a solution of Asp-N (2 μg/50 μL of 50 mM Bis-Tris-HCl buffer, pH 6.0), the reaction mixture was incubated at 37 °C for 2 h. The fragments were separated by HPLC (Figure 4) after addition of 50 μL of 10% TFA. The products were analyzed by MALDI-TOF MS and amino acid analyses (Table 1).

HPLC Comparison of a Digested Fragment and Two Possible Synthetic Fragments. The peptide fragment D4 (Figure 4), obtained by successive enzymatic digestion, was compared with two known synthetic fragments by using RP-HPLC on a Cosmosil 5PhT-300 (4.6 × 150 mm) phenyl column equipped with a Waters 510 binary gradient system.

Partial Reduction and Rapid Alkylation of [Tyr[32]]POI. Partial reduction and alkylation of [Tyr[32]]POI was performed according to the method of Gray (*20*). [Tyr[32]]POI (2.5 nmol) in 50 μL of 20% acetonitrile solution containing 0.1% TFA was reduced by dissolving the sample into 200 μL of TCEP solution (50 mM TCEP in 0.17 M citrate, pH 3, 15 °C) for specific periods. Reactions were terminated by injection into the RP-HPLC column, and the products were separated (Figure 8). The partially reduced fractions were collected directly into 200 μL of vigorously stirred supersaturated iodoacetamide solution (2.2 M in 0.5 M Tris-acetate, pH 8, containing 2 mM Na_2EDTA) for rapid alkylation. After the mixture was stirred for 30 s at room temperature, the reaction was terminated by addition of 400 μL of 0.5 M citric acid. The mixture was immediately injected into a Wakosil-II 5C_{18} (4.6 × 150 mm) column equipped with a 8020 HPLC system (Tosoh Co., Tokyo, Japan). Samples were eluted at 45 °C with 0.1% TFA in H_2O (solvent A) and 0.1% TFA in acetonitrile (solvent B). After injection of sample, the column was washed with 5% solvent B for 5 min at a flow rate of 1.5 mL/min and then the composition of solvent B was linearly raised from 5% to 50% over 45 min. The final products separated were examined by MALDI-TOF MS and automatic protein sequence analyses.

Molecular Modeling Based on Determined Disulfide Bridges. Molecular modeling of [Tyr[32]]POI was performed through energy minimizations and molecular dynamics (MD) simulations using AMBER 4.01 (*21*) on an NEC ACOS S3700 computer and NEC EWS4800/320 and Japan Computer Corp. JS 5/85 workstations. The united atom AMBER force field (*22*) with explicit treatment of heteroatom hydrogens was employed. For these calculations, a 12.0 Å cutoff for nonbonded interactions and a distance-dependent dielectric constant, $\epsilon = 4r$, to compensate for the lack of explicit solvent was used. Side-chain partial atomic charges on Asp, Glu, Arg, and Lys residues were reduced to give total charges of ±0.2 in order to reduce artifacts due to charge−charge interaction. In this preliminary conformational study, well-defined global minimum energy conformations were not explored, because no observable information except for intramolecular disulfide bridges was available at this point. Rather, we were concerned with identifying the overall topological preferences of this small peptide under the constraints of the three intramolecular disulfide bridges and conformational requirements of main-chain folding. The MD simulations were performed generally in two stages as follows.

First, initial conformations were randomly generated with the elimination of corrupted structures. The 50 initial structures were subjected to 300 cycles of steepest descent energy minimization and then 2000 steps of conjugated gradient minimization in order to avoid any high-energy interactions. Fifty derived coordinates were saved as initial conformations for use in the following MD simulations. In this stage, the six Cys residues were treated as six free cysteine residues. Next, these initial structures were heated to 300 K over a period of 50 ps without distance restraints, and then 300 ps restrained MD runs were performed in which three distance restraints between Sγ atoms in certain cysteine residues were added stepwise for every 100 ps MD run. The distance restraint function between two sulfur atoms was a parabola with a flat bottom between 2.00 and 2.04 Å that turned into a linear shape outside 2.16 Å with a maximum force of 100 kcal $Å^{-1}$ mol^{-1}. After another 50 ps dynamics run at 300 K with three disulfide restraints, the molecules were energetically minimized with the restrained force field.

In the second stage, these molecules were reconstructed by use of a LINK module in which all six cysteine residues were assessed as covalently linked cystine residues. Fifty energy-minimized coordinates were provided to LINK-generated structures by using an EDIT module. Next, the models were relaxed by conjugated gradient minimization and then subjected to the following simulated annealing calculations. The structures were equilibrated first at 1000 K for 5 ps, and then annealing is conducted by computing the MD trajectory while slowly cooling the system from 1000

to 300 K for 14 ps with a ramp of 2 fs/deg. Step size was set to 1 fs with the application of SHAKE (*23*) on all the bonds that contain hydrogen atom. This cycle was repeated 5 times. Next, the system was equilibrated at 300 K for 50 ps, after which the trajectory was sampled at 300 K in 10 ps intervals for 350 ps. The sampled structures were energy-minimized with conjugate gradients with a convergence criterion of 0.05 kcal/mol.

All the above procedures were applied for the analysis of the six possible disulfide-linking sequences. The schematic model for Cα trace of a typical structure is shown in the middle of Figure 9, in which the intramolecular disulfide bridges were linked in the order of Cys^{18}−Cys^{29}, Cys^{24}−Cys^{36}, and Cys^{11}−Cys^{25}. They showed distinctly lower energy ensembles than those obtained by other linking sequences.

POI Activity. The kinetics of the POI activities of native and synthetic peptides were determined by Lineweaver−Burk plots. PO was incubated in the presence and absence of either native or synthetic [Tyr^{32}]POI. The rate of dopa oxidation was determined in the presence of varying amounts of substrate by monitoring the changes in absorbance at 470 nm for dopachrome under the initial steady-state velocity at 25 °C. The reaction mixtures contained, in 3.0 mL of 50 mM potassium phosphate buffer, pH 6.0, PO, substrate (L-dopa, 0−4 mM), and [Tyr^{32}]POI (native or synthetic, 0−16.8 nM). Preincubation of the enzyme and inhibitor for 3 min prior to the addition of substrate was required for reproducible results. POI concentrations were determined by amino acid analyses. Housefly PO was purified from final instar larvae as an electrophoretically homogeneous protein by using a previously described method (*16*).

Mass Spectrometry. Matrix-assisted laser desorption/ionization time-of-flight mass spectrometry (MALDI-TOF MS) was performed on a Voyager-DE RP mass analyzer (PerSeptive Biosystems). Samples (about 2 pmol) were cocrystallized with α-cyano-4-hydroxycinnamic acid as a matrix. All the data were acquired in the reflector mode with delayed extraction. The molecular weights of native and synthetic [Tyr^{32}]POIs were examined on a JMS−HX/HX110A double-focusing mass spectrometer (Jeol, Tokyo) equipped with an electrospray ionization (ESI) ion source (Analytica, Branford, CT). About 100 pmol of native and synthetic [Tyr^{32}]POIs were dissolved in 10 μL of 0.2% TFA in acetonitrile/2-propanol/2-methoxyethanol/H_2O (1:1:1:1 v/v/v/v), and the solution was infused into the ESI ion source at a flow rate of 1 μL/min.

Amino Acid Composition Analysis. For amino acid composition analysis, about 30 pmol of sample lyophilized in small siliconized glass tubes were hydrolyzed under reduced pressure at 105 °C for 24 h in the gas phase of 5.7 M HCl containing 1% phenol. The hydrolysates were derivatized by phenyl isothiocyanate and examined on a Pico-Tag column (3.9 × 150 mm) equipped in a M600 multisolvent delivery system (Waters) according to the method reported by Bidlingmeyer et al. (*24*). All the data were processed on a 805 chromatogram data station (Waters). Half-cystine residues were identified as a cysteic acid as follows. Samples (approximately 15 pmol) lyophilized in siliconized tubes were subjected to performic acid oxidation. The samples were dissolved in 10 μL of freshly prepared performic acid solution (*25*) and incubated for 10 h at 0 °C. The residues were subjected to amino acid composition analyses as described above after two cycles of dissolution in 50 μL of H_2O and lyophilization.

Amino Acid Sequence Analyses. Automatic Edman degradation was carried out in a Shimadzu PPSQ-10 sequencer equipped for on-line phenylthiohydantoin (PTH-amino acids) analysis using an LC-10AS with a Wakosil WS−PTH column. Samples were applied to Sequa-Brene (Sigma) treated precycled glass fiber filters. PTH−Cys(Cam), PTH−Cys alkylated by iodoacetamide, was eluted between peaks of PTH−Ser and PTH−Thr, with an accompanying small peak [up to 15% of Cys(Cam), depending on the number of preceding cycles] of PTH-carboxymethylated cysteine, the deamidated product of Cys(Cam).

RESULTS

Synthesis of [Tyr^{32}]POI. Initial trials for the synthesis of [Tyr^{32}]POI through Fmoc strategy were unsuccessful. The stepwise coupling of protected amino acids by using TBTU [2-(1*H*-benzotriazol-1-yl)-1,1,3,3-tetramethyluronium tetrafluoroborate]/HOBt system produced a considerable number of defective peptides. Moreover, the major product cleaved from the polystyrene support gave a mass value of 4186.1 in its reduced form, a value that was 18 mass units less than expected. Air oxidation of this peptide gave a major product that displayed a different elution pattern and retention time from the native [Tyr^{32}]POI on coelution HPLC analysis. However, incubation of this peptide in 1% ammonium bicarbonate solution produced two peaks with the expected molecular mass values. The smaller peak, which eluted at a later retention time, was identified to be the native [Tyr^{32}]-POI. Asp-N digestion of these two peptides and subsequent mass analyses showed that the major product cleaved from the resin was a cyclized imide containing peptide at Asp^4. Such a product might be formed by repetitive treatments with deblocking solution (20% piperidine in DMF). The employment of HOBt-buffered deblocking solution (*17*), as well as the optimization of the repetitive couplings by use of HATU, and the appropriate time periods for individual steps, finally permitted the synthesis of complete linear peptide in reasonable yield. The air oxidation of linear peptide in 100 mM Tris-acetate (pH 7.5) at 4 °C produced essentially a unique product (Figure 1a), which was extensively purified by RP-HPLC as described (*19*) (Figure 1b). Oxidative folding of the peptide was temperature-sensitive. Addition of the mixture of reduced and oxidized glutathione increased the yields of misfolded peptides (data not shown). The final purified peptide was identified by both ESI and MALDI-TOF mass spectrometry, amino acid analysis (Table 1), and automatic Edman analysis (data not shown), and was confirmed to be identical to the native [Tyr^{32}]POI by coelution HPLC analysis (Figure 1c). Furthermore, the Lineweaver−Burk plots of dopa oxidation by larval PO in the presence of native or synthetic [Tyr^{32}]POI showed that both peptides inhibited PO-catalyzed oxidation of dopa in a competitive manner. The apparent K_i values determined in this study were 9.9 nM for synthetic [Tyr^{32}]POI and 11 nM for native [Tyr^{32}]POI, respectively, which showed that [Tyr^{32}]-POI synthesized in this study is comparable to native [Tyr^{32}]-POI isolated from pupae of the housefly.

Strategy for Assignment of Disulfide Bridges. The strategy used for establishing the disulfide array of [Tyr^{32}]POI is

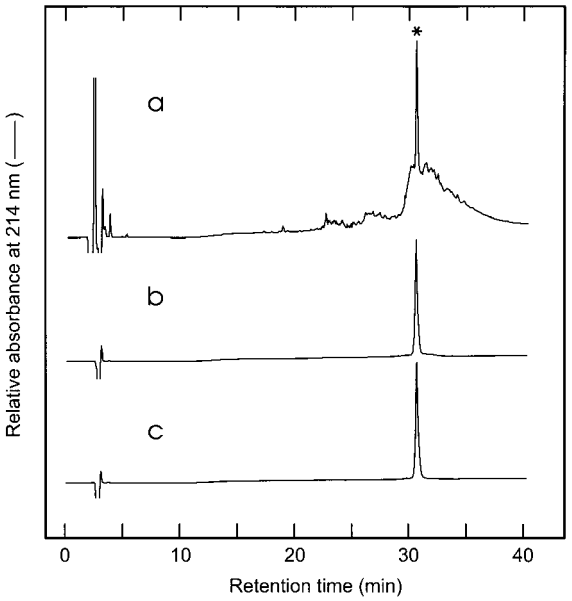

FIGURE 1: RP-HPLC analyses of synthetic and native [Tyr^{32}]POI. The elution profile of an air-oxidized solution of synthetic [Tyr^{32}]-POI is shown in panel a. The peak labeled by the asterisk was extensively purified as shown in panel b. The equimolar mixture of purified [Tyr^{32}]POI and native [Tyr^{32}]POI was eluted as shown in panel c. The peptides were eluted on a Cosmosil 5C_{18}AR-300 column (4.6 × 150 mm) at 45 °C equipped on a Shimadzu LC-10AD binary gradient system. Flow rate was 1.0 mL/min. Solvent A was 0.1% TFA in water and solvent B was 0.1% TFA in acetonitrile. Gradient conditions: 5% solvent B for the first 5 min and a linear 5−25% gradient of solvent B for additional 35 min.

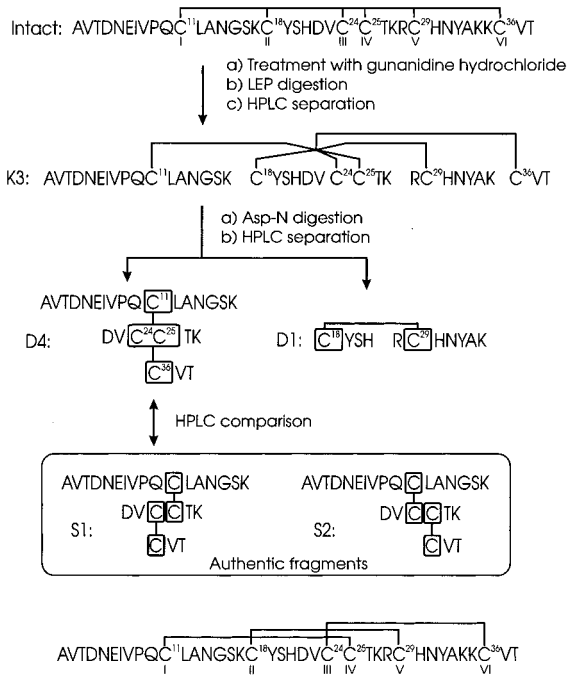

FIGURE 2: Strategy for determination of the disulfide bridges in [Tyr^{32}]POI. Intact [Tyr^{32}]POI was subjected to digestion by LEP as described in Materials and Methods. The products were separated by RP-HPLC (Figure 3) and characterized by amino acid analyses and MALDI-TOF MS (Table 1). One of these fragments, K3, was further digested by Asp-N (Figure 4). The fragment D4 containing adjacent disulfide pairings was compared with two authentic fragments synthesized (S1 and S2). Structures of these peptides having alternative disulfide pairs are enclosed in a large box. The cascadelike topology of the determined disulfide array in [Tyr^{32}]-POI is indicated at the bottom. The roman numerals shown under the sequence denote the relative order of six Cys residues from N terminus.

summarized in Figure 2. The presence of an adequate number of Lys and Asp residues suggested that enzymatic hydrolysis of the peptide by LEP and Asp-N in tandem would separate all the Cys residues except for adjacent Cys^{24} and Cys^{25} (D1 and D4 in Figure 2). For assignment of the disulfide linkages on these Cys residues, the fragment was compared with authentic peptides synthesized (S1 and S2; see below). Analytical data of the peptides are summarized in Table 1.

Proteolytic Digestion. Pretreatment of the peptide with 4 M guanidine hydrochloride at 70 °C was found to be crucial for subsequent LEP hydrolysis since POI is resistant to digestion under conventional conditions. [Tyr^{32}]POI was

Table 1: Amino Acid Compositions[a] and Mass Values[b] of Native and Synthetic [Tyr^{32}]POIs and the Fragment Peptides

	[Tyr^{32}]POI		digested peptides							authentic peptides	
residue	native	synthetic	K1	K2	K3	D1	D2	D3	D4	S1	S2
Asp/Asn	5.20 (5)	5.32 (5)	5.02 (5)	4.95 (5)	4.90 (5)	1.02 (1)	2.06 (2)	4.10 (4)	4.07 (4)	4.11 (4)	4.02 (4)
Glu/Gln	2.11 (2)	2.20 (2)	2.04 (2)	1.94 (2)	2.07 (2)	nd[c] (0)	2.10 (2)	2.03 (2)	1.97 (2)	2.03 (2)	1.94 (2)
Ser	1.89 (2)	2.06 (2)	1.93 (2)	1.90 (2)	1.86 (2)	0.95 (1)	1.01 (1)	0.94 (1)	0.97 (1)	1.22 (1)	0.97 (1)
Gly	1.07 (1)	1.12 (1)	1.03 (1)	1.03 (1)	1.06 (1)	nd (0)	1.06 (1)	1.04 (1)	1.00 (1)	0.94 (1)	1.00 (1)
His	1.92 (2)	2.11 (2)	1.86 (2)	1.99 (2)	1.88 (2)	2.01 (2)	nd (0)	nd (0)	nd (0)	nd (0)	nd (0)
Arg	0.94 (1)	1.08 (1)	1.03 (1)	0.98 (1)	1.03 (1)	0.99 (1)	nd (0)	nd (0)	nd (0)	nd (0)	nd (0)
Thr	2.91 (3)	3.16 (3)	2.90 (3)	3.03 (3)	2.87 (3)	nd (0)	1.88 (2)	1.96 (2)	2.82 (3)	2.81 (3)	2.82 (3)
Ala	3	3	3	3	3	1	1	1	2	1	2
Pro	0.99 (1)	1.03 (1)	1.01 (1)	0.95 (1)	1.04 (1)	nd (0)	0.95 (1)	1.02 (1)	0.99 (1)	1.02 (1)	0.99 (1)
Tyr	1.91 (2)	2.00 (2)	1.95 (2)	1.97 (2)	1.92 (2)	1.95 (2)	nd (0)	nd (0)	nd (0)	nd (0)	nd (0)
Val	3.84 (4)	4.11 (4)	3.79 (4)	3.80 (4)	4.05 (4)	nd (0)	2.94 (3)	2.88 (3)	3.83 (4)	3.93 (4)	3.83 (4)
Cys[c]	5.37 (6)	5.54 (6)	5.77 (6)	5.56 (6)	5.38 (6)	2.08 (2)	3.77 (4)	3.72 (4)	3.86 (4)	3.84 (4)	3.86 (4)
Ile	1.02 (1)	1.03 (1)	0.95 (1)	0.97 (1)	0.93 (1)	nd (0)	0.98 (1)	1.00 (1)	0.93 (1)	0.98 (1)	0.93 (1)
Leu	1.08 (1)	1.06 (1)	1.01 (1)	1.02 (1)	0.99 (1)	nd (0)	1.02 (1)	0.97 (1)	0.98 (1)	0.97 (1)	1.04 (1)
Lys	4.12 (4)	4.37 (4)	4.05 (4)	4.10 (4)	3.25 (3)	1.03 (1)	2.07 (2)	2.10 (2)	2.03 (2)	2.02 (2)	2.03 (2)
yield[e] (pmol)			120	551	708	520	135	67	310		
$[M+H]^+$	4197.5 ± 0.2 (4197.8)	4197.6 ± 0.2 (4197.8)	4252.5 (4252.8)	4234.1 (4233.8)	4123.8 (4123.6)	1396.6* (1396.6*)	2243.3 (2243.6)	2472.5 (2472.8)	2744.0 (2744.1)	2744.3 (2744.1)	2744.4 (2744.1)

[a] Values were calculated as moles per mole of Ala. Numbers in parentheses indicate theoretical values. [b] $[M + H]^+$, mass value of quasi-molecular ion. Numbers in parentheses indicate calculated values based upon average residue weights except for D1, which is based upon monoisotopic residue mass. [c] nd, not detected. [d] Values of Cys were determined as cysteic acid. Samples were treated with performic acid prior to analyses (see Material and Methods). [e] Yields indicate the recovery from 1.4 nmol of [Tyr^{32}]POI.

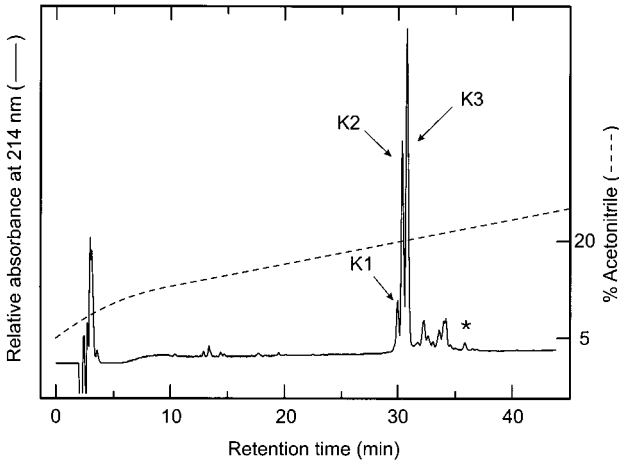

FIGURE 3: RP-HPLC separation of the LEP digest of intact [Tyr^{32}]-POI. Approximately 1.4 nmol of LEP-digested [Tyr^{32}]POI was separated on a Develosil ODS−UG-5 column (4.6 × 150 mm) at 35 °C equipped on a Waters 510 binary gradient system. Solvents and flow rates were as in Figure 1. Gradient conditions: 5−13% solvent B in first 10 min using a convex curve and 13−25% solvent B linearly for following 30 min. The major products are labeled as K1, K2, and K3. The small peak indicated by an asterisk was determined to be undigested [Tyr^{32}]POI.

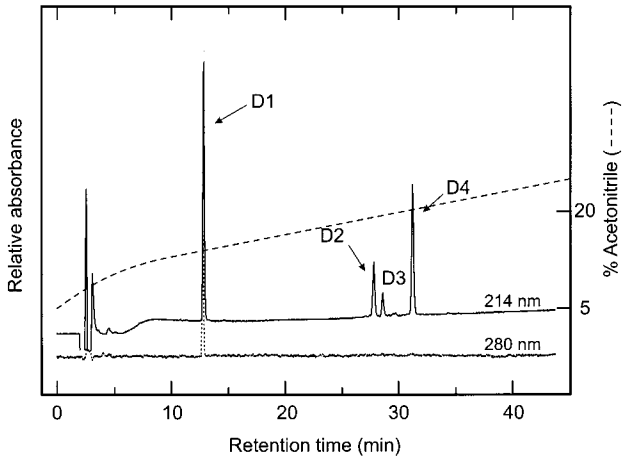

FIGURE 4: Separation of Asp-N digest of the LEP fragment K3 (Figure 3). Fragment K3 (560 pmol) was digested by endoproteinase Asp-N and the products were separated by HPLC as in Figure 3. Solid and dotted lines denote relative absorbance at 214 and 280 nm, respectively.

digested for 3 h, and the digest was separated by RP-HPLC as shown in Figure 3. LEP digestion yielded three major peaks, K1, K2, and K3, with several minor products eluting after the major peaks. Analyses of the major products indicated that the peptide was nicked at the carboxyl sites of Lys^{17}, Lys^{27}, and Lys^{34} for K1 and at Lys^{17} and Lys^{27} for K2, and K3 corresponded to the peptide K1 lacking Lys^{35} (Figure 2). The data also indicate that three Cys residues (Cys^{18}, Cys^{24}, and Cys^{25}) in the second fragment of K3 (Cys^{18}−Lys^{27}) are not connected to one another within this fragment.

During the course of LEP digestion, K1 and K2 were concertedly generated along with consumption of intact peptide. Meanwhile, K2 was gradually converted to K3. However, it was found that increasing the incubation time or the enzyme-to-substrate ratio actually reduced the yield of K3 and enhanced the production of minor peaks following K3. MALDI-TOF MS analyses of the minor peaks revealed that these were the peptides where disulfide scrambling occurred. Incubation of the peptide with LEP in neutral or basic buffer, suitable for LEP digestion, greatly reduced the yield of peak K3 and enhanced the disulfide scrambling.

To assign the peptide fragment connecting to Cys^{18}, the four-fifths peptide of K3 was further subjected to Asp-N digestion and the reaction mixture was separated as shown in Figure 4. The nicked peptide K3 was divided into two types of fragments: aromatic and hydrophilic fragment D1, and aliphatic and relatively hydrophobic fragments D2, D3, and D4. The fragment D1 was identified to be the peptide (C^{18}YSH) (RC^{29}HNYAK) by amino acid and mass spectrometric analyses (Table 1). The result that D1 is the only peptide containing aromatic residues among four Asp-N fragments is also confirmed by the chromatogram monitored at 280 nm. Thus a disulfide pair between Cys^{18} and Cys^{29} was established.

As in the case of LEP digestion, a decrease in selectivity was observed in Asp-N proteolysis at pH 6. Cleavage at the N-terminal side of Glu^{6} was observed in D2. The fragment D4 was not hydrolyzed at the peptide bond between Thr^{3} and Asp^{4}. The small peak D3 corresponds to the peptide that has been hydrolyzed at Asp^{4} in fragment D4. Again, prolonged incubation and proteolysis at neutral or basic pH yielded complex mixtures due to disulfide exchange. Therefor, to identify the adjacent disulfide pairs, the fragment peptide D4 was used for the subsequent comparative experiments with authentic peptides.

Synthesis of Authentic POI Fragments. Figure 5 shows a scheme for synthesis of peptide **S1**. This peptide possesses one of two possible combinations of disulfide pairs in peptide D4. Synthesis of the linear peptides **1**, **3**, and **6** was performed without difficulty. However, addition of HOBt to the deblocking reagent was required for peptide **1** to suppress cyclized imide formation after Fmoc-Asp(O*t*Bu)-OH was coupled at position 4. To prepare peptide **2**, we used an *in situ* one-pot conversion approach during the deprotection step. Here the Trt group at Cys in peptide **1** was quantitatively replaced with 2-thiopyridyl group by addition of 2,2′-dithiodipyridine to the final deprotection and cleavage cocktail instead of ethanedithiol (see Materials and Methods). Although the mixture lacked scavengers for free thiol, side reactions such as addition of Trt or tertiary butyl groups to sulfhydryl of Cys in peptide **2** were not observed. The removal of excess reagent and 2-thiopyridone generated together with the other compounds (scavenger-protecting group adducts, etc.) was easily accomplished by washing the white precipitate with diethyl ether. The purity of the obtained peptide was determined by HPLC and MALDI-TOF MS analyses, and the product was subjected to the next step without further purification. Intermolecular disulfide formation between peptide **2** and **4** in phosphate buffer quantitatively gave product **5**, which was purified by HPLC. The final product, **S1**, was successfully obtained by simultaneous iodine oxidation of **5** and **6** in 0.1 M HCl/methanol. Undesired symmetric homodimer formation of peptide **5** was suppressed by using an excess amount of peptide **6**. In addition, peptide **S2**, a counterpart of **S1**, was synthesized from peptide **3′**, a peptide that has the opposite combination of sulfhydryl protecting groups [DVC^{24}(Trt)C^{25}(Acm)TK]. The yields of two authentic peptides, which were purified by HPLC (Figure 6, Table 1), were calculated to be

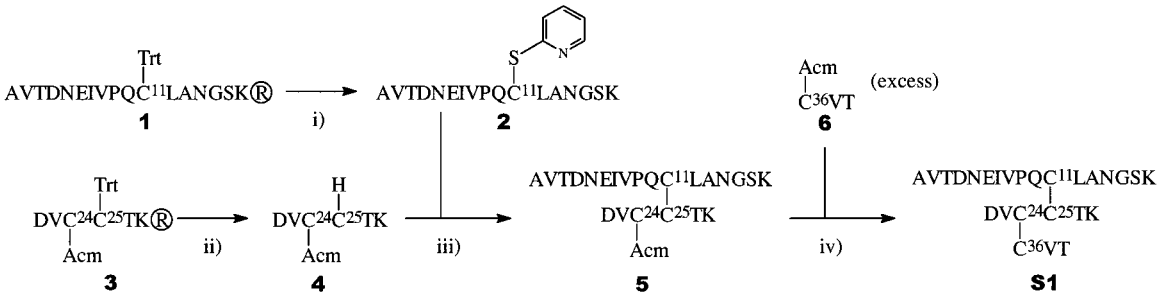

FIGURE 5: Scheme for synthesis of an authentic peptide S1. The symbol ® denotes polystyrene support used for solid-phase syntheses. The protecting groups, other than those of Cys, are omitted. (i) Deprotection and resin cleavage: TFA/thioanisole/*m*-cresol (80:17:3) containing 10 mol equivalent of 2,2′-dithiodipyridine. (ii) Deprotection and resin cleavage: TFA/thioanisole/*m*-cresol/ethanedithiol (80:12:2:6) under N_2 atmosphere. (iii) (a) Disulfide formation: phosphate buffer containing 1 mM Na_2EDTA, pH 6.0, 10 min, 25 °C under N_2 atmosphere; (b) HPLC purification. (iv) (a) I_2 in 0.1 M HCl, 5 min at 0 °C under N_2 atmosphere. (b) HPLC purification.

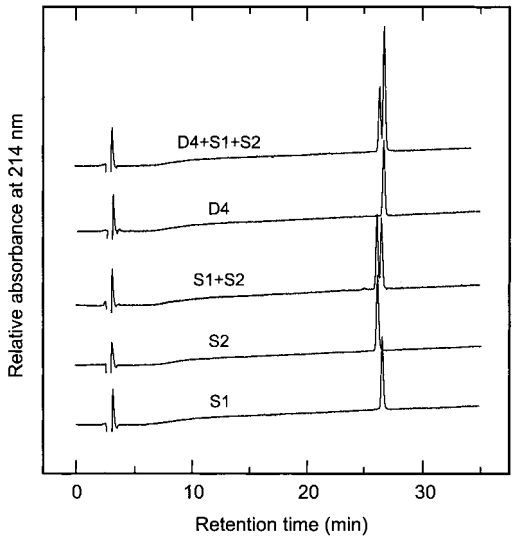

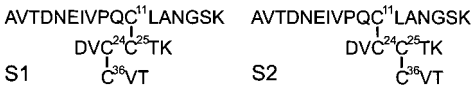

FIGURE 6: Assignment of the disulfide combination in proteolytic fragment D4 by coelution RP-HPLC analysis. Labels on each trace denote samples injected in the analyses. About 200 pmol of each peptide was eluted on a Cosmosil 5PhT-300 (4.6 × 150 mm) column at 35 °C. Solvents and flow rates were as in Figure 1. Gradient conditions: a linear 5−17% gradient of solvent B in 35 min. Two bottom traces, authentic peptides **S1** and **S2**, respectively; middle trace, coelution of **S1** and **S2** (1:1); second trace from top, proteolytic fragment D4; top trace, coelution of S1, S2, and D4 (1:1:1).

approximately 20% based on the amounts of compounds **3** and **3′** bound on the supports.

Assignment of Two Disulfide Pairings Including Adjacent Cys Residues. To assign the disulfide bonds connected to adjacent Cys residues, the proteolytic fragment D4 was compared with two authentic peptides **S1** and **S2** on RP-HPLC as shown in Figure 6. These peptides eluted as sharp single peaks (two bottom traces in Figure 6) which were well separated from each other as evidenced by coelution HPLC analysis of **S1** and **S2** (middle trace in Figure 6). The peptide **S1**, which has cross-connectivity of disulfides, eluted after the peptide with parallel connectivity (**S2**). The equimolar mixture of the two fractions was then co-injected with the same amount of the fragment D4. As shown in the top of Figure 6, the proteolytic fragment D4 coeluted with peptide **S1**; therefore, we establish the disulfide arrangement in fragment D4 to be Cys^{11}−Cys^{25} and Cys^{24}−Cys^{36}.

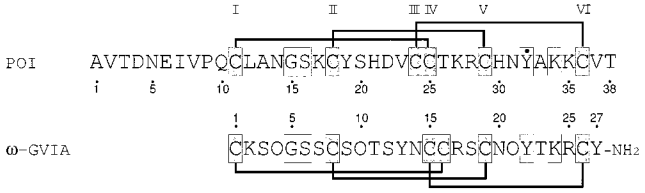

FIGURE 7: Comparison of amino acid sequences and disulfide configurations of housefly POI and *ω*-conotoxin GVIA from *Conus geographus* (*28*). The two peptides were aligned in order to maximize the overlapping of the Cys residues (shown in shaded boxes). Identical residues between two peptides are enclosed by a box. The characters Y crowned with dot and O denote dopa and 4-*trans*-hydroxyprolyl residue, respectively. The roman numerals shown above the sequence denote the relative order of the six Cys residues from the N terminus.

On the basis of the evidence presented, we demonstrate that the cystine connectivity in [Tyr^{32}]POI is Cys^{11}−Cys^{25}, Cys^{18}−Cys^{29}, and Cys^{24}−Cys^{36} (Figure 7). The cascadelike topology of these disulfides in [Tyr^{32}]POI, namely, I−IV, II−V, and III−VI (Figure 7), is identical with that of *ω*-conotoxin GVIA (Figure 7) (*26*), which was initially proposed to constitute the inhibitor cystine-knot structural family (*12*, *13*).

Partial Reduction of [Tyr^{32}]POI by Water-Soluble Phosphine. To further confirm the disulfide pairings in POI, we tried another orthogonal method reported by Gray (*20*). TCEP, tris(2-carboxyethyl)phosphine, which is a water-soluble reagent that can reduce disulfide bonds in peptides under acidic conditions, possesses the potential reduction without scrambling. In the case of [Tyr^{32}]POI, a small peak (R1), corresponding to 3% of the original intact material, emerged immediately after addition of the reducing agent (Figure 8b). This peak was identified as [Tyr^{32}]POI that was reduced at Cys^{11} and Cys^{25} as determined by sequencing of the S-alkylated peptide (see Materials and Methods). This initial reduction event also supports the disulfide pairing between Cys^{11} and Cys^{25}. Soon after a quick rise of peak R1, several unexpected peaks burst within 2 min of reduction (Figure 8c). The emergence of more than six peaks, besides the intact and fully reduced peptides, following the appearance of R1 strongly suggests that disulfide framework of POI cooperatively breaks down on the rapid scrambling, even at pH 3, once the disulfide between Cys^{11} and Cys^{25} is reduced.

Structure Simulation by Using Molecular Dynamics and Energy Minimization Based on Determined Disulfide Bridging Patterns. Since information on other peptides functionally

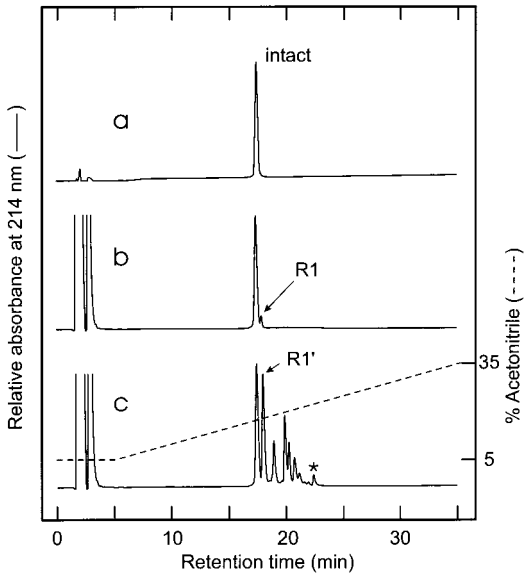

FIGURE 8: Partial reduction of [Tyr^{32}]POI. Approximately 2.5 nmol of synthetic [Tyr^{32}]POI (panel a) was reduced in 40 mM TCEP at pH 3, 15 °C. The reaction mixtures were separated on a Cosmosil 5C$_{18}$AR column (4.6 × 150 mm) at 55 °C. Solvents and flow rates were as in Figure 1. Gradient conditions: 5% solvent B in the first 5 min and a linear 5−35% gradient of solvent B for another 30 min. The peak R1, which was identified to be [Tyr^{32}]POI reduced at Cys^{11} and Cys^{25}, appeared within seconds (panel b) and soon after was followed by a burst of many peaks (panel c, enlarged in the vertical axis). Along with the propagation of these products, peak R1 changed to R1′ that contained a peptide reduced at Cys^{11} and Cys^{29}. The small peak labeled with an asterisk was identified to be the peptide in fully reduced form.

similar to POI is currently unavailable, we tried to construct a model of POI based on the disulfide connectivity. Cystine residues of POI are spread with roughly proportional spaces within the 26 C-terminal residues that contains the putative active site, Tyr^{32} (dopa^{32}). Therefore, molecular modeling based on the cystine connectivity should provide an approximate outline of the overall folding of POI as well as further information on its unique structural and functional character. We employed molecular dynamics and energy minimization procedures by using AMBER force field, where an extra pseudo-energy term was added to form correct pairings of sulfur atoms of Cys residues. Calculations were started with 50 random conformations.

The first trial, in which all disulfide restraints were simultaneously added to linear peptides, resulted in unfavorable highly strained conformations in which minimizations of these structures were crushed (data not shown). To overcome this problem, we employed a procedure where each single disulfide restraint was added step-by-step, and all possible permutations for the addition of disulfide restraints were examined. Interestingly, the final structures obtained were highly sensitive to the order of restraints added and only a specific sequence, first, Cys^{18}−Cys^{29}, second Cys^{24}−Cys^{36}, and third Cys^{11}−Cys^{25}, gave an energetically acceptable ensemble of conformations. The main-chain folding of a typical result produced by this procedure is shown in a schematic model (Figure 9). Calculations without disulfide restraints gave poor results, since all sulfur atoms that were not in the proper distance were unable to make disulfides.

DISCUSSION

Disulfide bonds in most cystine-clustered peptides play an essential role for providing a stable scaffold necessary for many biological functions. Therefore, the determination of disulfide pairings provides indispensable information for understanding unique structures of functional relevance. Moreover, correct knowledge of disulfide arrangement is important for a variety of experimental studies. Such studies include the design of flexible schemes for the preparation of synthetic peptides and related analogues, as well as for the analysis of solution and crystal structures.

POI is a novel class of dopa-containing cystine-rich peptide that inhibits PO with extraordinary potency. We studied the disulfide connectivity using synthetically prepared peptides because POI is present in low abundance in the housefly. Specifically, we used [Tyr^{32}]POI as the target because it had been demonstrated that dopa^{32} can be generated by oxidation of Tyr^{32} in vivo following intramolecular disulfide formation (*11*). In vitro, oxidative folding of synthetic [Tyr^{32}]POI gave a unique product corresponding to the native peptide with reasonable yield. In contrast, synthetic linear POI including

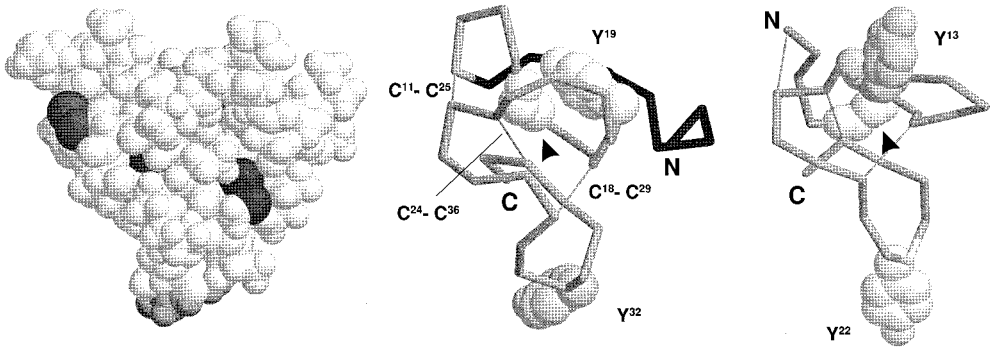

FIGURE 9: Schematic representations of the main-chain foldings of [Tyr^{32}]POI (middle) and ω-conotoxin GVIA (right). Traces of Cα atoms and disulfide bridges are indicated by thick and thin lines. The N and C termini of these peptides are labeled with N and C. The N-terminal residues preceding the cystine core of [Tyr^{32}]POI are densely hatched. Gly residues in the first intercystine sequences are shown by spheres and indicated by arrowheads. The side-chain atoms of Tyr residues, which form geographical counterparts between two peptides, are shown by shaded spheres. A space-filling model of [Tyr^{32}]POI is also depicted from an identical viewpoint as the middle model to show the bulk arrangement of exposed and buried Cys residues (left). Sulfur atoms and side-chain atoms of Tyr^{19} (buried) and Tyr^{32} are shaded heavily and lightly, respectively. The structure of [Tyr^{32}]POI shown in this figure is derived from the typical coordinates of ensembles from molecular dynamics and energy minimization calculations based on the determined cystine connectivities. The coordinates of ω-conotoxin GVIA (1CCO) were retrieved from the Protein Data Bank (*33*). The first structure in 1CCO was used for this presentation. The diagrams were generated by RASMOL (*34*).

dopa[32] resulted in complex mixture of inconsistent disulfide pairings (data not shown).

For the determination of disulfide pairings of [Tyr[32]]POI, we employed a composite procedure, in which the fragments containing disulfide bonds were separated by enzymatic hydrolysis and the fragments containing tandem Cys residues were compared to synthesized authentic peptides. One of these adjacent disulfides was confirmed by the orthogonal method, i.e., partial reduction at acidic pH followed by analysis of rapidly alkylated peptides. In addition, automatic Edman analysis of native POI also gave consistent results on the recovery of di-PTH-cystines (data not shown). Although the disulfide pattern of [Tyr[32]]POI was ultimately determined, the tendency for disulfide scrambling made a reliable assignment difficult. During the enzymatic digestions, the rates of disulfide exchange were kinetically controlled by keeping the reaction pH much lower than the ordinary conditions as well as by minimizing the time periods for reactions. Interestingly, the tendency for disulfide exchange was more evident in the intact form. Digestion of intact peptide by LEP required strict conditions to suppress scrambling. This was not the case for the nicked peptide (Figures 3 and 4). The relative stability of the nicked peptides suggests that the fragility of disulfides was attributable to an inherent character of intact POI. Furthermore, the persistence of synthetic fragments **S1** and **S2** in neutral buffer, and the rapid scrambling of the cystine framework observed during partial reduction, even at pH 3, also supports this thought. However, the POI resisted chemical reduction by 10 mM TCEP (a concentration where most cystine-containing peptides are reduced), implying a cryptic nature for the disulfides in POI. After chemical reduction of specific Cys residues, Cys[11] and Cys[25], we observed a massive shuffling of all the disulfide linkages in POI. The reduction of these Cys residues, which are supposed to be on the molecular surface in a strained POI structure, appears to cause the molecules to "burst" open, resulting in exposure of the other internal disulfide linkages. It is known that positively charged residues located close by or adjacent to Cys greatly enhance the rate constants in disulfide exchange reactions up to a 10^6-fold range (*27*). Abundance of His, Arg, and Lys just preceding or following Cys except for the initially reduced Cys[11] and Cys[25] may explain the cooperatively rapid disruption of the disulfide framework of POI (Figure 7).

The mode of disulfide bridges of POI was determined to follow a cascadelike topology with I−IV, II−V, and III−VI connectivity (Figure 7). This topological character is often found in toxins from snail and spider as well as protease inhibitors and defense peptides from plants and insects (*13*). Such peptides are known to be the members of a inhibitor cystine-knot structural family. Despite their functional differences and very low primary sequence homology, these peptides share a common cystine motif and a tertiary structure incorporating a pseudo-cystine-knot and a triple-stranded β-sheet (*12, 13*). Among these peptides, POI shows remarkable similarity to those of snail toxins consisting of a 4-loop framework in terms of not only topology of disulfides but also the geography of cystine residues (*28*). Comparisons of the sequences and disulfide pattern of POI with ω-conotoxin GVIA, a well-characterized toxin of snails (refs *26, 29* and the references therein), also revealed a characteristic abundance of both basic and hydroxyl moieties distributed over the molecules. Furthermore, Gly at the center of the first intercystine sequence (between Cys[I] and Cys[II]), which has been the only non-Cys residue absolutely conserved among all the ω-conotoxins (*28*) and requisite to form a type II β-turn in the conotoxin structures (*30, 31*), was also found in POI. This suggests a resemblance in main-chain folding between POI and ω-conotoxins.

The schematic models of main-chain folding of [Tyr[32]]-POI (Figure 9) shows roughly a triple-stranded β-sheet with a $+2x, -1$ topology and a pseudo-cystine-knot. The striking similarity in main-chain folding and spatial arrangement of disulfide bridges between [Tyr[32]]POI and ω-conotoxin GVIA previously reported (1CCO; *29*) and the occurrence of Gly[15] at a β-turn-like structure in the simulated coordinates of POI also rationalize this model. The model contains few ordered hydrogen bonds; however, the requirement of predenaturalization by guanidine hydrochloride for proteolytic hydrolysis indicates the presence of ordered intramolecular hydrogen bonds in POI as noted in ω-conotoxin GVIA (*29*). In the model, three disulfide bridges are lined up from the surface of the molecule to the inside as zipping the main chain compact (middle panel in Figure 9); one side of the aligned disulfides, Cys[11]−Cys[25], is exposed in contrast to the other two buried disulfide bridges (left panel in Figure 9). Specific reduction of the disulfide bond between Cys[11] and Cys[25] and the accompanying disruption of cystine framework observed in this study might be due to the unfastening motion of these three disulfides. Similar behavior of disulfide bridges was reported on ω-conotoxin GVIA, in which an all-or-none melting of reduction was observed (*20*). This is also consistent with the structure simulation studies where acceptable folding was accomplished only by a specific order of disulfide formation, in which Cys[11] and Cys[25] was restrained at the end of the disulfide linking sequence.

In conclusion, we propose that the novel peptide POI is a newly found member of the inhibitor cystine-knot structural family. The spatial arrangement of two Tyr residues in our model of POI, where Tyr[32] juts out from the bottom of the largest loop in contrast to buried Tyr[19], is consistent with biological function, as only Tyr[32] is enzymatically oxidized to a dopa residue in vivo. It is intriguing that these two Tyr residues of POI are located at the corresponding sites of two of the three Tyr in ω-conotoxin GVIA (Tyr[13] and Tyr[22], Figure 9) and that Tyr[13] of conotoxin corresponds to Tyr[19] of POI. Functionally, Tyr[13], but not Tyr[22], of ω-conotoxin GVIA is a crucial residue for the binding to N-type Ca^{2+} channel (*32*). Such structural analogy between POI and ω-conotoxin GVIA, together with the known diversity of biological function of other related peptides within the inhibitor cystine-knot structural family, suggests that POI may have a broader biological distribution as well as have other roles besides the regulation of intact PO.

ACKNOWLEDGMENT

We are grateful to Dr. H. Fukuda (Nihon PerSeptive Ltd.) for his continuous support on improving 9050 equipment and its protocols. We thank Dr. Dennis J. Grab (Saga University) for carefully reading the manuscript, Mr. S. Sakamoto (Saga University) for his assistance in structural calculations, and Drs. M. Kusunoki (Institute for Protein

Research, Osaka University) and H. Eto (Information Processing Center, Saga University) for utilization of computational facilities. We also thank Mr. I. Konoike and Mr. K. Kimura (Milbon Corporation) for their continued encouragement.

REFERENCES

1. Mason, H. S. (1948) *J. Biol. Chem. 172*, 83−99.
2. Lerch, K. (1983) *Mol. Cell. Biochem. 52*, 125−138.
3. Brunet, P. C. J. (1980) *Insect Biochem. 10*, 125−138.
4. Hopkins, T. L. (1982) *Science 217*, 364−366.
5. Sugumaran, M. (1988) *Adv. Insect Physiol. 21*, 179−231.
6. Brookman, J. L., Ratcliffe, N. A., and Rowley, A. F. (1989) *Insect Biochem. 19*, 47−57.
7. Ashida, M., Doke, K., and Onishi, E. (1974) *Biochem. Biophys. Res. Commun. 57*, 1089−1095.
8. Tsukamoto, T., Ishiguro, M., and Funatsu, M. (1986) *Insect Biochem. 16*, 573−581.
9. Aspán, A., and Söderhäll, K. (1991) *Insect Biochem. 21*, 363−373.
10. Tsukamoto, T., Ichimaru, Y., Kanegae, N., Watanabe, K., Yamaura, I., Katsura, Y., and Funatsu, M. (1992) *Biochem. Biophys. Res. Commun. 184*, 86−92.
11. Daquinag, A. C., Nakamura, S., Takao, T., Shimonishi, Y., and Tsukamoto, T. (1995) *Proc. Natl. Acad. Sci. U.S.A. 92*, 2964−2968.
12. Narasimhan, L., Singh, J., Humblet, C., Guruprasad, K., and Blundell, T. (1994) *Nat. Struct. Biol. 1*, 850−852.
13. Pallaghy, P. K., Nielsen, K. J., Craik, D. J., and Norton, R. S. (1994) *Protein Sci. 3*, 1833−1839.
14. Abdelmoty, I., Albericio, F., Carpino, L. A., Foxman, B. M., and Kates, S. A. (1994) *Lett. Pept. Sci. 1*, 57−67.
15. Burns, J. A., Butler, J. C., Morgan, J., and Whitesides, G. M. (1991) *J. Org. Chem. 56*, 2648−2650.
16. Hara, T., Tsukamoto, T., Maruta, K., and Funatsu, M. (1989) *Agric. Biol. Chem. 53*, 1387−1393.
17. Lauer, J. L., Fields, C. G., and Fields, G. B. (1994) *Lett. Pept. Sci. 1*, 197−205.
18. Ellman, G. L. (1959) *Arch. Biochem. Biophys. 82*, 70−77.
19. Sato, T., Ito, H., Takeda, Y., and Shimonishi, Y. (1992) *Bull. Chem. Soc. Jpn. 65*, 938−940.
20. Gray, W. R. (1993) *Protein Sci. 2*, 1732−1748.
21. Pearlman, D. A., Case, D. A., Caldwell, J. C., Seibel, G. L., Singh, U. C., Weiner, P., and Kollman, P. A. (1991) AMBER 4.0, University of California, San Francisco.
22. Weiner, S. J., Kollman, P. A., Case, D. A., Singh, U. C., Ghio C., Alagona, G., Profeta, S., Jr., and Weiner, P. (1984) *J. Am. Chem. Soc. 106*, 765−784.
23. Gunsteren, W. F., and Berendsen, H. J. C. (1977) *Mol. Phys. 34*, 1311−1327.
24. Bidlingmeyer, B. A., Cohen, S. A., and Tarvin, T. L. (1984) *J. Chromatogr. 336*, 93−104.
25. Hirs, C. H. W. (1967) *Methods Enzymol. 11*, 59−62.
26. Nishiuchi, Y., Kumagaye, K., Noda, Y., Watanabe, T. X., and Sakakibara, S. (1986) *Biopolymers 25*, S61−S68.
27. Snyder, G. H., Cennerazzo, M. J., Karalis, A. J., and Field, D. (1981) *Biochemistry 20*, 6509−6519.
28. Olivera, B. M., Miljanich, G. P., Ramachandran, J., and Adams, M. E. (1994) *Annu. Rev. Biochem. 63*, 823−867.
29. Pallaghy, P. K., Duggan, B. M., Pennington, M. W., and Norton, R. S. (1993) *J. Mol. Biol. 234*, 405−420.
30. Davis, J. H., Bradley, E. K., Miljanich, G. P., Nadasdi, L., Ramachandran, J., and Basus, V. J. (1993) *Biochemistry 32*, 7396−7405.
31. Lew, M. J., Flinn, J. P., Pallaghy, P. K., Murphy, R., Whorlow, S. L., Wright, C. E., Norton, R. S., and Angus, J. A. (1997) *J. Biol. Chem. 272*, 12014−12023.
32. Kim, J. I., Takahashi, M., Ogura, A., Kohno, T., Kudo, Y., and Sato, K. (1994) *J. Biol. Chem. 269*, 23876−23878.
33. Bernstein, F. C., Koetzle, T. F., Williams, G. J., Meyer, E. E., Jr., Brice, M. D., Rodgers, J. R., Kennard, O., Shimanouchi, T., and Tasumi, M. (1977) *J. Mol. Biol. 112*, 535−542.
34. Sayle, R. A., and Milner-White, E. J. (1995) *Trends Biochem. Sci. 20*, 374.

BI9819834